

# Constructive topological classification of real algebraic surfaces<sup>1</sup>

E. Fortuna<sup>a</sup>, P. Gianni<sup>a</sup> and D. Luminati<sup>b</sup>

<sup>a</sup>*Dipartimento di Matematica, Università di Pisa, via Buonarroti 2, I-56127 Pisa, Italy*

<sup>b</sup>*Dipartimento di Matematica, Università di Trento, v. Sommarive n. 14 - loc. Povo, I-38050 Trento, Italy*

---

## Abstract

We present an algorithm to compute the topology of a non-singular real algebraic surface  $S$  in  $\mathbb{R}P^3$ , that is the number of its connected components and a topological model for each of them. Our strategy consists in computing the Euler characteristic of each connected component by means of a Morse-type investigation of  $S$  or of a suitably constructed compact affine surface. This procedure can be used to determine the topological type of an arbitrary non-singular surface; in particular it extends an existing algorithm applicable only to surfaces disjoint from a line.

---

## 1 Introduction

The aim of this paper is to give an algorithm to determine the topological type of a non-singular real algebraic surface  $S$  of degree  $d$  in the real projective space  $\mathbb{R}P^3$ , computing the number of the connected components of  $S$  and characterizing topologically each of them.

Our procedure will rely on some basic classical results concerning topological and algebraic surfaces that we now briefly recall; for a proof of these facts we refer the reader to Massey (1991) and, for instance, to Viro (1998).

If the degree  $d$  is even, the surface and all its connected components are orientable. By the topological classification theorem for surfaces, we know that

---

*Email addresses:* fortuna@dm.unipi.it (E. Fortuna), gianni@dm.unipi.it (P. Gianni), luminati@science.unitn.it (D. Luminati).

<sup>1</sup> This research was partially performed with the contribution of M.U.R.S.T. and of Eurocontract HPRN-CT-2001-00271

any compact connected orientable surface is homeomorphic to the connected sum of a sphere and  $g$  tori, i.e. it is homeomorphic to a torus with  $g$  holes, with  $g \geq 0$  (meaning that a torus with 0 holes is a sphere). The number  $g$ , called *genus*, is a complete topological invariant for connected orientable surfaces, hence it is possible to characterize topologically each connected component of an even-degree surface computing its genus or, equivalently, its *Euler characteristic*  $\chi = 2 - 2g$ , which is always an even integer.

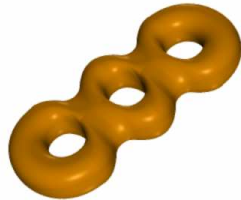


Fig. 1. A torus with 3 holes

If  $d$  is odd,  $S$  contains exactly one non-orientable connected component, while all the other components are orientable. The topological classification theorem for surfaces ensures that any compact connected non-orientable surface is homeomorphic to the connected sum of either a projective plane or a Klein bottle and a compact connected orientable surface of genus  $g$ ; the Euler characteristic is then respectively either  $\chi = 1 - 2g$  or  $\chi = -2g$ , that is either odd or even. Since a surface with an even Euler characteristic may be either orientable or non-orientable, the only knowledge of the characteristic is in general not sufficient to determine the topological model of a compact connected surface, unless we know whether it is orientable or not. In our case however the situation is simpler because the Euler characteristic of a non-orientable connected surface contained in  $\mathbb{RP}^3$  is necessarily odd (for a proof, see Viro (1998), 1.3.A).

Thus, even if the degree is odd, the knowledge of the list of the Euler characteristics of the connected components of  $S$  determines the topological type of  $S$ , since any component having an even characteristic  $\chi$  is necessarily homeomorphic to the corresponding orientable model, that is to a torus with  $\frac{2-\chi}{2}$  holes, and the unique component having an odd characteristic  $\chi$  is homeomorphic to the connected sum of a projective plane and a torus with  $\frac{1-\chi}{2}$  holes.

The problem of the algorithmic determination of the topological type of a non-singular real projective algebraic surface has already been solved in Fortuna et al. (2003) for surfaces disjoint from a line (hence of even degree and orientable), in particular for all non-singular compact algebraic surfaces contained in  $\mathbb{R}^3$ . In this paper we will extend that result computing the topology of an arbitrary non-singular projective surface  $S$ ; the basic idea is proving that the topological type of  $S$  can be algorithmically recovered from the one of a suitable compact algebraic surface  $\tilde{S}$  in  $\mathbb{R}^3$ , and then computing the topology

of  $\widehat{S}$  by means of the algorithm presented in Fortuna et al. (2003). Section 2 is devoted to construct  $\widehat{S}$  starting from  $S$  and to relate their topological types from a theoretical point of view. In Section 3 we briefly recall the compact-case algorithm of the cited paper and present an improvement to it; then, in Section 4, we turn the results of Section 2 into constructive procedures and present the general-case algorithm. The last section contains some examples and also some remarks on the computational aspects and on the implementation of the algorithm.

## 2 Reduction to the compact affine case

Let  $S$  be a non-singular real projective surface in  $\mathbb{RP}^3$  defined by the equation  $F(x, y, z, t) = 0$ , where  $F$  is a homogeneous polynomial of degree  $d$  with real coefficients. By saying that  $S$  is non-singular we mean that no point in  $\mathbb{RP}^3$  annihilates  $F$  and all its first partial derivatives, while the complex zero-set defined by  $F$  may contain non-real singular points. In this section we will see how the topological characterization of  $S$  can be reduced to the topological investigation of a compact affine surface  $\widehat{S}$  in  $\mathbb{R}^3$ .

The projective space  $\mathbb{RP}^3$  can be seen as the quotient space of the 3-sphere  $S^3$  with respect to the antipodal equivalence relation which identifies every pair of diametrically opposite points in  $S^3$ , relation induced by the map  $\pi : S^3 \rightarrow \mathbb{RP}^3$  associating to any point  $(x, y, z, t) \in S^3$  the point of homogeneous coordinates  $[x, y, z, t]$  in  $\mathbb{RP}^3$ . In this way  $S^3$  turns out to be a 2-sheeted covering space of  $\mathbb{RP}^3$ . Consider in  $S^3$  the non-singular surface

$$\widetilde{S} = \pi^{-1}(S) = \{(x, y, z, t) \in \mathbb{R}^4 \mid F(x, y, z, t) = 0\} \cap S^3.$$

If we denote by  $ap : S^3 \rightarrow S^3$  the antipodal map defined by  $ap(v) = -v$ , evidently  $ap(\widetilde{S}) = \widetilde{S}$ ; more precisely  $ap$  transforms each connected component of  $\widetilde{S}$  into a connected component, acting therefore as an involution on the set  $\mathcal{F}$  of the connected components of  $\widetilde{S}$ .

Taking into account the action of  $ap$  on the connected components of  $\widetilde{S}$ , we can split  $\mathcal{F}$  as the union of  $\mathcal{F}_1$  and  $\mathcal{F}_2$ , where

$$\mathcal{F}_1 = \{\widetilde{T} \mid \widetilde{T} \in \mathcal{F}, ap(\widetilde{T}) = \widetilde{T}\} \quad \text{and} \quad \mathcal{F}_2 = \mathcal{F} \setminus \mathcal{F}_1.$$

In particular  $ap$  induces a pairing among the elements of  $\mathcal{F}_2$ .

If we consider the preimage of a connected component of  $S$  through the double covering  $\pi$ , we can immediately observe:

**Lemma 2.1** *Let  $Y$  be a connected component of  $S$  and let  $\tilde{Y} = \pi^{-1}(Y)$ . Then*

- i)  $\chi(\tilde{Y}) = 2 \chi(Y)$
- ii) *if  $\tilde{Y}$  is not connected, then it has exactly two connected components  $\tilde{Y}_1$  and  $\tilde{Y}_2$ , each homeomorphic to  $Y$ , and  $ap(\tilde{Y}_1) = \tilde{Y}_2$*
- iii) *if  $Y$  is non-orientable, then  $\tilde{Y}$  is connected and  $\tilde{Y} \in \mathcal{F}_1$ .*

*Proof.* i) and ii) follow from the fact that  $\pi|_{\tilde{Y}} : \tilde{Y} \rightarrow Y$  is a 2-sheeted covering of  $Y$ .

iii)  $\tilde{Y}$  is surely orientable. Then  $\tilde{Y}$  is connected, because otherwise, by part ii), each of its two connected components would be homeomorphic to  $Y$ , which is non-orientable. Since  $ap(\tilde{Y}) = \tilde{Y}$ , then  $\tilde{Y} \in \mathcal{F}_1$ .  $\square$

As explained in the introduction, in order to compute the topological type of  $S$  it is sufficient to count the connected components of  $S$  and to determine them topologically by means of their Euler characteristics. Next proposition shows how these data can be recovered from the knowledge of the connected components of  $\tilde{S}$  and of the sets  $\mathcal{F}_1$  and  $\mathcal{F}_2$ :

**Proposition 2.2** *Assume that*

$$\mathcal{F}_1 = \{\tilde{T}_1, \dots, \tilde{T}_m\} \quad \text{and} \quad \mathcal{F}_2 = \{\tilde{T}_{m+1}, \dots, \tilde{T}_q, ap(\tilde{T}_{m+1}), \dots, ap(\tilde{T}_q)\}.$$

*Then  $S$  is homeomorphic to  $M(\frac{\chi(\tilde{T}_1)}{2}) \cup \dots \cup M(\frac{\chi(\tilde{T}_m)}{2}) \cup \tilde{T}_{m+1} \cup \dots \cup \tilde{T}_q$ , where*

- a) *if  $r$  is an even integer,  $M(r)$  denotes the orientable connected surface with Euler characteristic  $r$ , that is a torus with  $\frac{2-r}{2}$  holes,*
- b) *if  $r$  is an odd integer,  $M(r)$  denotes the non-orientable connected surface with Euler characteristic  $r$ , that is the connected sum of a projective plane and a torus with  $\frac{1-r}{2}$  holes.*

*Proof.* If  $\tilde{T}_j \in \mathcal{F}_1$ , then  $Y = \pi(\tilde{T}_j)$  is a connected component of  $S$  such that  $\pi^{-1}(Y) = \tilde{T}_j$  and  $\chi(\tilde{T}_j) = 2 \chi(Y)$ .

If  $\tilde{T}_j \in \mathcal{F}_2$ , then  $Y = \pi(\tilde{T}_j)$  is homeomorphic to  $\tilde{T}_j$  and  $\pi^{-1}(Y) = \tilde{T}_j \cup ap(\tilde{T}_j)$ .  $\square$

**Remark 2.3** Note that, in the previous proposition, it is not necessary to know the exact pairing  $ap$  among the components in  $\mathcal{F}_2$ . Namely, by Lemma 2.1 we know that, if a surface appears in  $\mathcal{F}_2$ , then  $\mathcal{F}_2$  contains an even number of surfaces homeomorphic to it. It is then sufficient to insert half of them in the list of the topological models of the components of  $S$  coming from  $\mathcal{F}_2$ .  $\square$

A first observation in the direction of computing  $\mathcal{F}_1$  and  $\mathcal{F}_2$  can be made considering for instance the intersection of  $\tilde{S}$  with the  $ap$ -invariant subset

$$\widetilde{W} = \{z = 0\} \cap S^3.$$

Since  $\widetilde{W}$  disconnects  $S^3$  into two parts transformed each into the other by  $ap$ , if  $\widetilde{T} \in \mathcal{F}_1$ , then necessarily  $\widetilde{T} \cap \widetilde{W} \neq \emptyset$ ; in other words, if  $\widetilde{T} \cap \widetilde{W} = \emptyset$ , then  $\widetilde{T} \in \mathcal{F}_2$ . Observe however that the converse is not true, so that a more accurate investigation is needed to split  $\mathcal{F}$ .

If  $\widetilde{W}$  is transversal to  $\widetilde{S}$ , then  $\widetilde{W} \cap \widetilde{S}$  is a non-singular curve and  $ap$  induces, by restriction, an involution also on the set  $\widetilde{\mathcal{O}}$  of the connected components of  $\widetilde{W} \cap \widetilde{S}$ .

For any  $\omega \in \widetilde{\mathcal{O}}$  we will denote by  $\widetilde{T}(\omega)$  the connected component of  $\widetilde{S}$  containing  $\omega$ . Using the fixed notations, we get the following first characterization useful to split  $\mathcal{F}$  into  $\mathcal{F}_1 \cup \mathcal{F}_2$ :

**Proposition 2.4**  *$\widetilde{T} \in \mathcal{F}_1$  if and only if there exist  $\omega_1, \omega_2 \in \widetilde{\mathcal{O}}$  (possibly coinciding) such that  $\widetilde{T}(\omega_1) = \widetilde{T}(\omega_2) = \widetilde{T}$  and  $ap(\omega_1) = \omega_2$ .*

*Proof.* If  $\widetilde{T} \in \mathcal{F}_1$ , then  $\widetilde{T} \cap \widetilde{W} \neq \emptyset$ . If  $\omega$  is a connected component of  $\widetilde{T} \cap \widetilde{W}$ , then also  $ap(\omega)$  is a connected component of  $\widetilde{T} \cap \widetilde{W}$ , since  $ap(\widetilde{T}) = \widetilde{T}$  and  $ap(\widetilde{T} \cap \widetilde{W}) = \widetilde{T} \cap \widetilde{W}$ . Then  $\widetilde{T}(\omega_1) = \widetilde{T}(ap(\omega_1)) = \widetilde{T}$ . Conversely, let  $x \in \omega_1 \subset \widetilde{T}$ . Then  $ap(x) \in \omega_2 \subset \widetilde{T}$  and also  $ap(x) \in ap(\widetilde{T})$ . Then  $\widetilde{T}$  and  $ap(\widetilde{T})$  are connected components having  $ap(x)$  as a common point; hence  $ap(\widetilde{T}) = \widetilde{T}$  and therefore  $\widetilde{T} \in \mathcal{F}_1$ .  $\square$

Proposition 2.2 transforms our original problem into that of studying the surface  $\widetilde{S}$  in  $S^3$ , its connected components and the splitting  $\mathcal{F}_1 \cup \mathcal{F}_2$ , which can be detected by means of the criterion given in Proposition 2.4. As a matter of fact, we can actually perform this investigation not working on  $\widetilde{S}$ , but on a compact affine surface  $\widehat{S}$  in  $\mathbb{R}^3$  homeomorphic to it and obtained via stereographic projection.

Namely, up to an affine translation, we can assume that  $[0, 0, 0, 1] \notin S \subset \mathbb{RP}^3$ ; hence  $N = (0, 0, 0, 1) \notin \widetilde{S}$  and  $(0, 0, 0, -1) \notin \widetilde{S}$ . Then the stereographic projection  $\varphi : S^3 \setminus \{N\} \rightarrow \mathbb{R}^3$ , given by  $\varphi(x, y, z, t) = (\frac{x}{1-t}, \frac{y}{1-t}, \frac{z}{1-t})$ , is a homeomorphism transforming  $\widetilde{S}$  into the compact affine surface  $\widehat{S} = \varphi(\widetilde{S}) \subset \mathbb{R}^3$ , which is the zero-set of  $F \circ \varphi^{-1}$  and does not contain the origin.

If we denote  $X = (x, y, z) \in \mathbb{R}^3$ , then  $\varphi^{-1}(X) = (\frac{2X}{\|X\|^2+1}, \frac{\|X\|^2-1}{\|X\|^2+1})$  and hence

$$(F \circ \varphi^{-1})(X) = F \left( \frac{2X}{\|X\|^2+1}, \frac{\|X\|^2-1}{\|X\|^2+1} \right) = \frac{1}{(\|X\|^2+1)^d} F(2X, \|X\|^2-1),$$

where  $d = \deg F$ , and  $\|X\|^2 = x^2 + y^2 + z^2$ . Thus, if we set

$$G(X) = F(2X, \|X\|^2-1),$$

then  $G = 0$  is a polynomial equation for the algebraic surface  $\widehat{S} \subset \mathbb{R}^3$ . Observe that, if  $S$  (and hence  $\widetilde{S}$ ) is a non-singular surface, since  $\varphi$  is a biregular isomorphism between  $S^3 \setminus \{N\}$  and  $\mathbb{R}^3$ , also the image surface  $\widehat{S}$  is non-singular. Note also that, since  $F(0, 0, 0, 1) \neq 0$ , then  $F$  contains a monomial  $ct^d$  with  $c \neq 0$ ; hence  $\deg G = 2d$ .

A straightforward computation shows that the antipodal map  $ap$  in  $S^3$  is conjugated to the map  $inv = \varphi \circ ap \circ \varphi^{-1} : \mathbb{R}^3 \setminus \{0\} \rightarrow \mathbb{R}^3 \setminus \{0\}$  given by  $inv(X) = -\frac{X}{\|X\|^2}$ .

Let  $\widehat{W} = \varphi(\widetilde{W} \setminus \{N\}) = \{z = 0\} \subset \mathbb{R}^3$ . We will denote by  $\widehat{\mathcal{F}}, \widehat{\mathcal{F}}_1, \widehat{\mathcal{F}}_2, \widehat{\mathcal{O}}$  the sets of components corresponding through  $\varphi$  to  $\mathcal{F}, \mathcal{F}_1, \mathcal{F}_2, \mathcal{O}$  and, for any  $\omega \in \widehat{\mathcal{O}}$ , we will denote by  $\widehat{T}(\omega)$  the connected component of  $\widehat{S}$  containing  $\omega$ . In particular Proposition 2.4 turns into

**Proposition 2.5**  *$\widehat{T} \in \widehat{\mathcal{F}}_1$  if and only if there exist  $\omega_1, \omega_2 \in \widehat{\mathcal{O}}$  (possibly coinciding) such that  $\widehat{T}(\omega_1) = \widehat{T}(\omega_2) = \widehat{T}$  and  $inv(\omega_1) = \omega_2$ .*

### 3 The compact-case algorithm

In the next section we will describe a constructive procedure to compute the topology of an arbitrary non-singular real projective surface in  $\mathbb{RP}^3$ , generalizing the algorithm presented in Fortuna et al. (2003). Both for the previous algorithm and for the new general one, the core of the procedure is the topological determination of a non-singular compact affine surface in  $\mathbb{R}^3$ . In this section we will briefly recall, at least in its main steps, how the ‘‘Compact-Case-Algorithm’’ (for short CCA) works, referring to the original paper Fortuna et al. (2003) for most of the theoretical and algorithmic details. This gives us the opportunity to describe some situations that had not been considered in the previous paper, and also to present some modifications we have made to the original version of the algorithm, resulting in an improvement of the numerical stability of the whole procedure.

So, in the present section,  $S$  will denote a compact affine surface in  $\mathbb{R}^3$  defined by the polynomial equation  $G(x, y, z) = 0$ . We assume that  $S$  is non-singular, that is no point in  $S$  annihilates all the first partial derivatives of  $G$ .

To compute the topology of  $S$  we use as a basic tool Morse theory (see for instance Milnor (1963) or Hirsch (1976)), since, up to a generic linear change of coordinates, one can assume that the function  $p(x, y, z) = z$  projecting  $S$  to the  $z$ -axis is a Morse function and that distinct critical points correspond to distinct critical values. To check that  $p$  is a ‘‘good projection’’ in the previous sense, we need to compute the real critical points of  $p$  (that is the points in

$S$  where the first partial derivatives of  $G$  with respect to  $x$  and  $y$  vanish) and to test that all of them are non-degenerate. The non-singularity test and the computation of the critical points are the most delicate and time-consuming tasks in the whole algorithm; additional comments can be found in the final section.

After computing the (finitely many, non-degenerate) critical points for  $p$  on  $S$ , we can consider an interval  $[-N, N]$  containing all the critical values of  $p$  and subdivide it as  $[-N, N] = [-N, a_1] \cup [a_1, a_2] \cup \dots \cup [a_s, N]$  in such a way that each  $a_i$  is non-critical for  $p$  and each interval  $[a_i, a_{i+1}]$  contains only one critical value in its interior part.

The strategy for computing the topology of  $S$  consists in iteratively reconstructing the topology of the level surfaces  $S_{a_i} = p^{-1}([-N, a_i]) = S \cap \{z \leq a_i\}$  passing from one level  $a_i$  to the higher level  $a_{i+1}$ ; this is sufficient since  $S = S_N$ . By Morse theory, if  $[a_i, a_{i+1}]$  contains exactly one critical value  $c$  for  $p$ , with  $a_i < c < a_{i+1}$ , and  $k$  is the index of the corresponding non-degenerate critical point, then  $S_{a_{i+1}}$  is homotopically equivalent to the space obtained attaching a  $k$ -cell to  $S_{a_i}$ . This is sufficient for our aim, because homotopically equivalent spaces have the same homology groups and the same Euler characteristics.

The iterative step of the CCA algorithm requires to detect how the  $k$ -cell attaches to  $S_{a_i}$  and to reconstruct some data concerning the boundary of  $S_{a_{i+1}}$  starting from the corresponding data for the level surface  $S_{a_i}$ . In Fortuna et al. (2003) it is explained how the knowledge of these data allows us to compute the number of connected components of  $S_{a_{i+1}}$  and their topological types.

First of all we need to study the shape of the level curves  $C_{a_i} = p^{-1}(a_i) = S \cap \{z = a_i\}$ , whose connected components are the boundary components of the level surface  $S_{a_i}$ . Since the levels  $a_i$  are non-critical values for  $p$ , any level curve to be studied is a non-singular compact affine curve of even degree. Then all its connected components are ovals, i.e. each of them disconnects  $\mathbb{R}^2$  into two connected components, one homeomorphic to a disc and called the *interior part* of the oval, the other not bounded and called the *exterior part* of the oval. Recall also that an oval is called empty if no other oval is contained in its interior part; moreover a list  $[\omega_1, \dots, \omega_m]$  of ovals of a curve is called a *nest* of depth  $m$  if  $\omega_1$  is empty,  $\omega_i$  is contained in the interior part of  $\omega_{i+1}$  for all  $i = 1, \dots, m-1$  (and any other oval containing  $\omega_i$  contains also  $\omega_{i+1}$ ) and  $\omega_m$  is not contained in the interior part of any oval of the curve. The shape of any level curve is completely determined when the set of its nests is known.

The second main point in the iterative step of the algorithm is reconstructing the function  $\mu_{a_i}$  that associates to any oval  $\omega$  of the curve  $C_{a_i}$  the connected component  $\mu_{a_i}(\omega)$  of  $S_{a_i}$  containing  $\omega$  in its boundary. Observe first that, if an interval  $[a, b]$  contains no critical value, then  $C_b$  has as many ovals and

as many nests as  $C_a$  and it is easy to compute  $\mu_b$  starting from  $\mu_a$ . Namely, assume that  $P$  is a point *in the center of a nest*  $n$  of  $C_a$ , that is  $P$  is internal to the first (i.e. the innermost) oval of the nest and therefore internal to all the ovals of the nest. If we lift  $P$  up to the level  $b$  following a continuous path that does not intersect the surface, the endpoint  $P'$  of this path lies in the center of a nest  $N$  of  $C_b$  of the same depth as  $n$ . Then the  $k$ -th oval of  $N$  belongs to the boundary of the connected component of  $S_b$  that contains also the  $k$ -th oval of  $n$ . The choice of a point  $P$  in the center of a nest and the computation of the ovals containing  $P'$  can actually be performed, since we have added to the curve-algorithm two special functions:

- the function *findOvals*, given a point  $P \in \mathbb{R}^2$  and a curve  $C$ , returns the list of the ovals of  $C$  containing  $P$  ordered by inclusion starting from the innermost oval,
- the function *findPoint*, given an oval  $\omega$  of  $C$ , returns a point lying inside  $\omega$ , more precisely a point  $Q$  such that  $\omega$  is the first oval of the sequence *findOvals*( $Q$ ).

Just to fix notations, if  $R$  is a point in the plane  $\{z = a\}$  and  $b > a$ , we will denote by *roadMap*( $R, b$ ) the final point  $\alpha(1)$  of a continuous semialgebraic path  $\alpha : [0, 1] \rightarrow \{a \leq z \leq b\}$  such that  $\alpha(0) = R$ ,  $\alpha(1) \in \{z = b\}$  and  $\alpha([0, 1]) \cap S = \emptyset$ . Similarly, if  $b < a$ , we will denote by *invRoadMap*( $R, b$ ) the final point  $\beta(1)$  of a continuous semialgebraic path  $\beta : [0, 1] \rightarrow \{b \leq z \leq a\}$  fulfilling the same conditions as  $\alpha$  here above.

For intervals  $[a_i, a_{i+1}]$  containing a critical value, the method outlined above does not allow to fully compute the function  $\mu_{a_{i+1}}$  since there is not a bijective correspondence between the set of the ovals of  $C_{a_i}$  and the set of the ovals of  $C_{a_{i+1}}$ . In Fortuna et al. (2003) the authors proposed a way to develop the previous idea into a reconstructive procedure for  $\mu_{a_i}$  using an additional roadmap starting from a point next to the critical point. We are now able to propose a different method, still based on roadmaps, but which avoids the problems of precision due to the choice of a point sufficiently near the critical point. Let us start to illustrate this new method in details in the case of critical points of index 1, because this is the case presenting the widest range of situations.

To simplify our notations, we will describe how to compute  $\mu_b$  starting from  $\mu_a$  when  $[a, b]$  is an interval containing in its interior part exactly one critical value  $c$ , which is the image of a unique critical point  $P \in S$ . If  $P$  has index 1,  $S_b$  is obtained from  $S_a$  by attaching a 1-cell to the boundary of  $S_a$ . There are two possible situations: either the 1-cell is attached to a single oval of the level curve  $C_a$ , or it is attached to two distinct ovals of it. It is easy to realize which is the situation, because in the former  $C_b$  has more ovals than  $C_a$ , in the latter it has fewer ovals. Since the two situations are nearly symmetric, we will describe the details of the reconstructive procedure for  $\mu_a$  only in the



first case.

Figure 2 shows the possible situations that can occur attaching a 1-cell to an oval  $\eta$  of the curve  $C_a$ , which, in the passage through the critical value, gives origin to two distinct ovals  $\omega_1, \omega_2$  of the curve  $C_b$ .

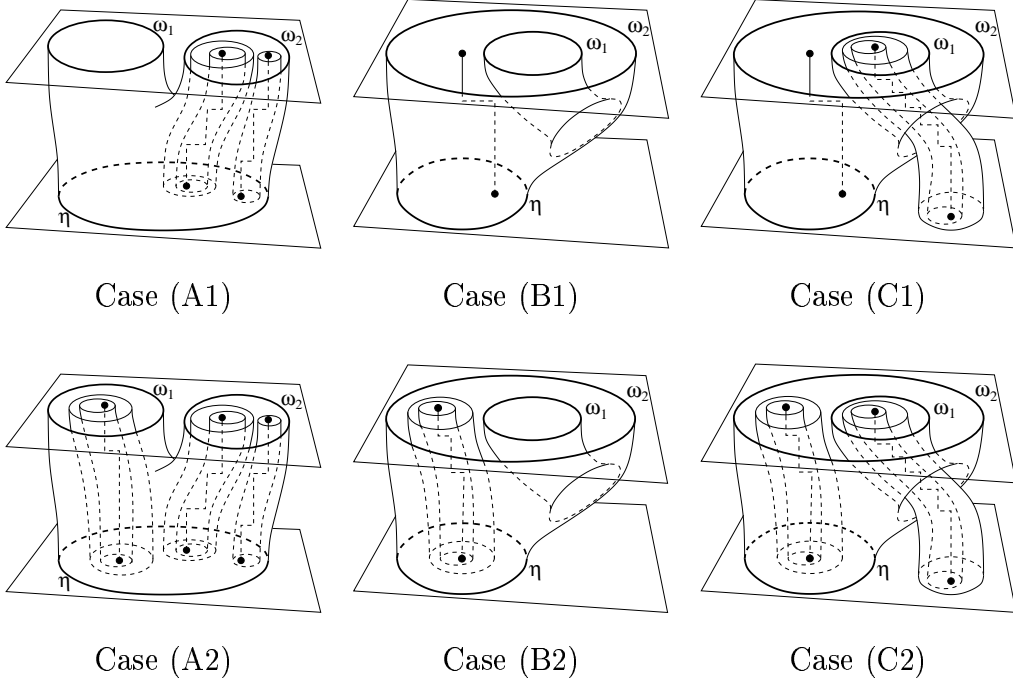


Fig. 2. List of possible situations when  $C_b$  has more ovals than  $C_a$

We can assume that, by the previous iterative step, we already know the list  $[(P_1, n_1), \dots, (P_k, n_k)]$ , where  $n_1, \dots, n_k$  are the nests of the curve  $C_a$  and  $P_i$  is a point in the center of the nest  $n_i$ . Denote by  $[N_1, \dots, N_s]$  the list of the nests of  $C_b$ . Moreover, for any list  $l$ , denote by  $l.i$  the  $i$ -th element of the list.

The essential step to compute the function  $\mu_b$  (and consequently to compute the topology of  $S_b$ ) is just computing, for  $i = 1, \dots, k$ ,

$$Q_i = \text{roadMap}(P_i, b) \quad \text{and} \quad Ov(Q_i) = \text{findOvals}(Q_i).$$

It may happen either that  $Ov(Q_i)$  coincides with a nest  $N_j$  of  $C_b$  (and then we say that  $N_j$  is reached through a roadmap) or not.

If  $n_i$  is a nest such that the list  $Ov(Q_i)$  contains as many elements as  $n_i$ , then  $\mu_b(Ov(Q_i).j) = \mu_a(n_i.j)$  for all  $j$ . In this way in particular we succeed in computing  $\mu_b$  for all ovals belonging to nests of  $C_b$  that contain neither of the ovals  $\omega_1, \omega_2$  originated from the splitting of the oval  $\eta$  of  $C_a$ . In order to complete the computation of  $\mu_b$ , it is necessary to detect  $\eta, \omega_1, \omega_2$ ; let us see how we can do that, first of all deciding in which of the cases (A1),  $\dots$ , (C2) of Figure 2 we are.

Start by comparing the integers  $k$  and  $s$ , that is the number of the nests respectively of  $C_a$  and  $C_b$ .

**Case 1) :  $s < k$ .**

Looking at Figure 2, the only case in which  $C_b$  has fewer nests than  $C_a$  is (C1). In this case there exists a unique  $P_i$  such that  $Q_i$  is not in the center of any nest of  $C_b$ . Then  $\omega_2 = Ov(Q_i).1$  and  $\eta = n_i.1$ . Moreover there exists at least one  $P_j$  such that  $Ov(Q_j)$  is a nest containing more ovals than  $n_j$ , precisely  $\# Ov(Q_j) = \# n_j + 2$ . Then  $\omega_2$  appears as one of the ovals in  $Ov(Q_j)$ : if  $\omega_2 = Ov(Q_j).r$ , then  $\omega_1 = Ov(Q_j).(r - 1)$ .

**Case 2) :  $s = k$ .**

The possible cases in which  $C_b$  has as many nests as  $C_a$  are (B1), (A2) and (C2).

- If there exists a (unique) nest  $N \in \{N_1, \dots, N_s\}$  not reached through a roadmap (i.e.  $N \notin \{Ov(Q_i)\}_{i=1, \dots, k}$ ), then we are in case (B1). In this situation there exists a unique nest  $n_i$  such that  $Ov(Q_i)$  is not a nest of  $C_b$ ; then  $\omega_1 = N.1$ ,  $\omega_2 = N.2$  and  $\eta = n_i.1$ .
- If all the nests of  $C_b$  are reached through roadmaps (in other words if  $\{Ov(Q_i)\}_{i=1, \dots, k} = \{N_1, \dots, N_s\}$ ) and, for all  $i$ , we have  $\# Ov(Q_i) = \# n_i$ , then we are in case (A2). The ovals  $\eta, \omega_1, \omega_2$  can be found inspecting how ovals common to distinct nests in  $C_a$  lift through roadmaps. Namely, in case (A2) there exist at least two nests  $n_i \neq n_j$  such that, for some integers  $r$  and  $m$ , we have  $n_i.r = n_j.m$  but  $Ov(Q_i).r \neq Ov(Q_j).m$ . Then  $\eta = n_i.r (= n_j.m)$ , while  $\omega_1 = Ov(Q_i).r$  and  $\omega_2 = Ov(Q_j).m$ .
- Otherwise we are in case (C2). Denote by  $L_2$  the list of the nests  $n_i$  such that  $\# Ov(Q_i) = \# n_i + 2$ , and by  $L_0$  the list of the  $n_i$  such that  $\# Ov(Q_i) = \# n_i$ . Note that in case (C2), both  $L_2$  and  $L_0$  are non-empty. Let  $n_i$  be any element of  $L_2$  and let  $r$  be the smallest integer such that  $Ov(Q_i).r \in Ov(Q_j)$  for some  $n_j \in L_0$ . Then  $\omega_1 = Ov(Q_i).(r - 1)$  and  $\omega_2 = Ov(Q_i).r$ . Moreover if  $Ov(Q_i).r = Ov(Q_j).m$ , then  $\eta = n_j.m$ .

**Case 3) :  $s > k$ .**

The possible cases are (A1) and (B2). In both cases there exists a unique nest  $N \in \{N_1, \dots, N_s\}$  not reached through roadmaps, i.e.  $N \notin \{Ov(Q_i)\}_{i=1, \dots, k}$ . Then  $\omega_1 = N.1$ . To determine  $\eta$  and  $\omega_2$  we take  $Q$  in the interior part of  $\omega_1$  (for instance  $Q = findPoint(\omega_1)$ ) and compute  $P = invRoadMap(Q, a)$ . Let  $r = \# findOvals(Q)$  and  $m = \# findOvals(P)$  (possibly  $m = 0$ , if  $P$  is not contained in any oval of  $C_a$ ).

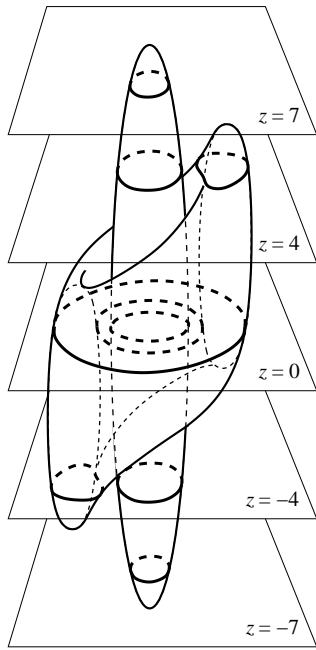
- If  $r = m$ , we are in case (A1) and  $\eta = findOvals(P).1$ . Once we have found a nest  $n_i$  such that  $\eta = n_i.j$ , then  $\omega_2 = Ov(Q_i).j$ .
- If  $r > m$ , we are in case (B2). This time  $\omega_2 = N.2$ . If  $\omega_2 = Ov(Q_i).j$ , then  $\eta = n_i.j$ .

We proceed in a similar way when a 1-cell is attached to two distinct ovals  $\omega_1$  and  $\omega_2$  of  $C_a$  that glue together into a single oval  $\eta$  of  $C_b$ . The oval  $\eta$  is in the boundary both of the connected component of  $S_b$  containing  $\omega_1$  and of the component containing  $\omega_2$ . This is the only case when two distinct connected components of  $S_a$  may glue together : if  $\mu_a(\omega_1) \neq \mu_a(\omega_2)$  (i.e.  $\omega_1$  and  $\omega_2$  bound distinct connected components of  $S_a$ ), then the distinct components  $\mu_a(\omega_1)$  and  $\mu_a(\omega_2)$  glue into a single connected component  $\mu_b(\eta)$  of  $S_b$ .

After the previous considerations, it should be clear how to reconstruct  $\mu_b$  when we pass through a critical point of index 0. In the case of index 2, it is sufficient to adapt the previous method preliminarily computing, by means of *findPoint*, a point  $Q_i$  in the center of each nest  $N_i$  of  $C_b$  and the corresponding point  $P_i = \text{invRoadMap}(Q_i, a)$ .

**Example.** Let  $S \subset \mathbb{R}^3$  be the surface defined by the equation

$$\begin{aligned} F(x, y, z) = & \frac{169}{6250}z^6 + \frac{1}{6250}(11154y^2 + 11141x^2 + 11059)z^4 - 4yz^3 + \\ & + \left(\frac{21801}{6250}y^4 + \left(\frac{42757}{6250}x^2 + \frac{1340243}{6250}\right)y^2 + \frac{3353}{1000}x^4 + \frac{107211}{500}x^2 - \frac{667}{8}\right)z^2 + \\ & + 256(1 - x^2 - y^2)yz + \frac{5408}{3125}y^6 + \frac{1}{3125}(15808x^2 - 1225408)y^4 + \\ & + \left(\frac{616}{125}x^4 - \frac{99216}{125}x^2 + \frac{46952}{5}\right)y^2 + \frac{8}{5}x^6 - \frac{2008}{5}x^4 + 9400x^2 - 9000 = 0. \end{aligned}$$



Since the projective closure of  $S$  in  $\mathbb{RP}^3$ , defined by the homogenized polynomial  $t^6 F(\frac{x}{t}, \frac{y}{t}, \frac{z}{t})$ , does not meet in real points the plane at infinity  $\{t = 0\}$ , then  $S$  is compact in  $\mathbb{R}^3$ . After testing that  $S$  is non-singular and that the projection  $p : S \rightarrow \mathbb{R}$ ,  $p(x, y, z) = z$ , is a Morse function, the algorithm computes 6 critical values contained in the interval  $[-10, 10]$ , which is subdivided as  $[-10, -7] \cup [-7, -4] \cup [-4, 0] \cup [0, 4] \cup [4, 7] \cup [7, 10]$  so that each subinterval contains exactly one critical value. By an abuse of language we will say that a critical value has index  $r$  if it is the image through  $p$  of a critical point of index  $r$ .

Each of the first two intervals  $[-10, -7]$  and  $[-7, -4]$  contains a critical value of index 0 and the level curve  $C_{-4}$  consists of two ovals each external to the other. The third critical value, lying in  $[-4, 0]$ , has index 1. Since  $C_0$  has only one nest of depth 3, then  $C_0$  has more ovals than  $C_{-4}$  (i.e. the 1-cell is attached to a single oval of  $C_{-4}$ ), but fewer nests, hence we are in Case (C1) of Figure 2. Lifting from level 0 to level 4, we pass through a critical value of index 1 and  $C_4$  has two nests, each of depth 1. Hence the 1-cell is attached to two distinct ovals of  $C_0$ , that we can

detect simply computing the endpoint  $Q = \text{roadMap}(P, 4)$  for a point  $P$  in the center of the unique nest of  $C_0$  and finding, using *findOvals*, the smallest oval of  $C_4$  containing  $Q$ . The investigation of the last two intervals  $[4, 7]$  and  $[7, 10]$ , each containing a critical value of index 2, allows us to realize that  $S$  has two connected components, respectively of Euler characteristic 0 and 2. Thus  $S$  is the disjoint union of a torus and a sphere.

#### 4 The general-case algorithm

In this section we want to see how we can algorithmically proceed to compute the topology of a non-singular real projective surface  $S$  defined by the equation  $F(x, y, z, t) = 0$ , with  $F$  a homogeneous polynomial of degree  $d$ . Recall that checking that  $S$  is non-singular means to check that the algebraic variety defined by the homogeneous ideal generated by all four partial derivatives of  $F(x, y, z, t)$  does not contain any real point, while complex singularities are allowed.

If  $S$  does not intersect (in real points) the line  $L = \{z = t = 0\}$ , we are in the situation when the topology of  $S$  can be studied using the algorithm presented in Fortuna et al. (2003). From now on, we will therefore assume that  $S \cap L \neq \emptyset$ , which for instance always occurs if the degree  $d$  is odd. In this situation, as we have already seen in Section 2, the topological determination of  $S$  can be reduced to studying the compact affine non-singular surface  $\hat{S} \subset \mathbb{R}^3$  defined by the equation  $G(x, y, z) = 0$  and to recognizing the sets of components  $\hat{\mathcal{F}}_1$  and  $\hat{\mathcal{F}}_2$ . The former task can be achieved applying to  $\hat{S}$  the algorithm CCA recalled in the previous section; thus, when CCA stops, we know the connected components of  $\hat{S}$  (or equivalently of  $\tilde{S}$ ) and their Euler characteristics.

In order to complete the topological determination of  $S$  we only need to compute the sets  $\hat{\mathcal{F}}_1$  and  $\hat{\mathcal{F}}_2$  recalling that, by Proposition 2.5,  $\hat{T}_j \in \hat{\mathcal{F}}_1$  if and only if there exist  $\omega_1, \omega_2 \in \hat{\mathcal{O}}$ , possibly coinciding, contained in the same connected component of  $\hat{S}$  and such that  $\text{inv}(\omega_1) = \omega_2$ . In particular all the components of  $\hat{S}$  not intersecting  $\widehat{W}$  necessarily belong to  $\hat{\mathcal{F}}_2$ . Thus, the further tasks we have to perform algorithmically are to determine the list  $\hat{\mathcal{O}}$  of the connected components of the curve  $\hat{C}_0 = \widehat{W} \cap \hat{S} = \{G(x, y, 0) = 0\}$  and, for each oval  $\omega \in \hat{\mathcal{O}}$ , to recognize both the connected component of  $\hat{S}$  where it is contained and the corresponding oval  $\text{inv}(\omega)$ . Up to a translation of the surface  $S$ , we can assume that 0 is not a critical value for the projection  $p$  so that we can choose 0 as one of the non-critical levels  $a_i$  mentioned above. Thus  $\widehat{W}$  is transversal to  $\hat{S}$  and  $\hat{C}_0$  is non-singular. Since 0 appears among the levels  $a_i$ , at the corresponding iterative step the algorithm CCA applied to  $\hat{S}$  already performs the following tasks:

- T1. it computes the list  $\widehat{\mathcal{O}}$  of the ovals of  $\widehat{C}_0$  and the shape of  $\widehat{C}_0$ ; more precisely the function *nestsZero* returns a list  $[(P_1, n_1), \dots, (P_r, n_r)]$ , where  $n_1, \dots, n_r$  are the nests of  $\widehat{C}_0$  and  $P_i$  is a point internal to all the ovals of the nest  $n_i$ ,
- T2. it computes a function  $\mu_0 : \widehat{\mathcal{O}} \rightarrow \widehat{\mathcal{S}}$ , where  $\widehat{\mathcal{S}}$  denotes the set of the connected components of the level surface  $\widehat{S}_0 = \widehat{S} \cap \{z \leq 0\}$  and, for each oval  $\omega$  of the curve  $\widehat{C}_0$ ,  $\mu_0(\omega)$  is the connected component of  $\widehat{S}_0$  containing  $\omega$  in its boundary.

Note that if  $\omega_1, \omega_2 \in \widehat{\mathcal{O}}$  and  $\mu_0(\omega_1) = \mu_0(\omega_2)$ , then the connected components  $\widehat{T}(\omega_1)$  and  $\widehat{T}(\omega_2)$  of  $\widehat{S}$ , respectively containing  $\omega_1$  and  $\omega_2$ , coincide. On the contrary, if  $\mu_0(\omega_1) \neq \mu_0(\omega_2)$ , we can only be sure that  $\omega_1$  and  $\omega_2$  belong to different components of the level surface  $\widehat{S}_0$ . Nevertheless it may happen that the two components are then glued in  $\widehat{S}$  (and hence  $\widehat{T}(\omega_1) = \widehat{T}(\omega_2)$ ) when passing through a critical value  $> 0$  by the attachment of a 1-cell to two distinct ovals  $\sigma_1$  and  $\sigma_2$  of a level curve  $\widehat{C}_{a_i}$  such that  $\mu_{a_i}(\sigma_1)$  contains  $\omega_1$  and  $\mu_{a_i}(\sigma_2)$  contains  $\omega_2$  (see for instance Figure 3). This is simple to detect by means of the procedure described in Section 3.

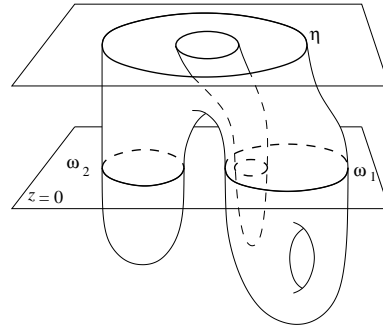


Fig. 3. *Distinct components of  $\widehat{S}_0$  that glue in  $\widehat{S}$ .*

The only left question is therefore, for each oval  $\omega$  of  $\widehat{C}_0$ , determining the oval  $inv(\omega)$ . Next proposition shows how this can be done using the mentioned functions *findOvals* and *findPoint*. Observe that the restriction of  $inv$  to  $\widehat{W} \setminus \{0\}$  is an inversion transforming points next to 0 to points “next to infinity” and viceversa. If we identify  $\widehat{W}$  with  $\mathbb{R}^2$  and denote by  $\overline{\mathbb{R}^2}$  the extended plane obtained adjoining  $\infty$  to  $\mathbb{R}^2$ , then we can consider  $inv$  as a continuous function on  $\overline{\mathbb{R}^2}$  such that  $inv(0) = \infty$  and  $inv(\infty) = 0$ .

**Proposition 4.1** *Let  $\omega$  be an oval of  $\widehat{C}_0$  and denote by  $int(\omega)$  the interior part of  $\omega$ .*

- a) *If  $0 \notin int(\omega)$ , then  $findOvals(inv(findPoint(\omega))) = [inv(\omega), \dots]$ .*
- b) *If  $findOvals(0) = [\omega_0, \dots, \omega_p]$ , then  $inv(\omega_i) = \omega_{p-i}$  for all  $i = 0, \dots, p$ .*
- c) *If  $[\omega_1, \dots, \omega_m]$  is a nest of  $\widehat{C}_0$  and  $j$  is the biggest index in  $\{1, \dots, m\}$*

such that 0 is not internal to  $\omega_j$ , then

$$\text{findOvals}(\text{inv}(\text{findPoint}(\omega_1))) = [\text{inv}(\omega_1), \dots, \text{inv}(\omega_j), \dots].$$

*Proof.* a) Note that  $\text{inv}$  transforms each connected component of  $\overline{\mathbb{R}^2} \setminus \omega$  into a connected component of  $\overline{\mathbb{R}^2} \setminus \text{inv}(\omega)$ . If  $0 \notin \text{int}(\omega)$ , then 0 and  $\infty$  belong to the same component of  $\overline{\mathbb{R}^2} \setminus \omega$  and therefore also  $\text{inv}(0)$  and  $\text{inv}(\infty)$  belong to the same component of  $\overline{\mathbb{R}^2} \setminus \text{inv}(\omega)$ . Thus  $0 \notin \text{int}(\text{inv}(\omega))$ . By the same argument, if  $P \in \text{int}(\omega)$  (i.e.  $P$  and  $\infty$  lie in different components of  $\overline{\mathbb{R}^2} \setminus \omega$ ), then  $\text{inv}(P) \in \text{int}(\text{inv}(\omega))$ , so that  $\text{inv}(\text{int}(\omega)) = \text{int}(\text{inv}(\omega))$ . As a consequence, if we take  $P = \text{findPoint}(\omega)$ , then  $\text{inv}(P) \in \text{int}(\text{inv}(\omega))$ . Moreover  $\text{inv}(\omega)$  is the first oval containing  $\text{inv}(P)$ : otherwise, if there exists  $\omega'$  such that  $\text{inv}(P) \in \text{int}(\omega') \subset \text{int}(\text{inv}(\omega))$ , then by the same argument  $P \in \text{int}(\text{inv}(\omega')) \subset \text{int}(\omega)$ . This is impossible because, by the definition of  $\text{findPoint}$ ,  $\omega$  is the smallest oval containing  $P$ .

b) If  $0 \in \text{int}(\omega)$ , then  $0 \in \text{int}(\text{inv}(\omega))$ : otherwise, by a),  $0 \notin \text{int}(\text{inv}(\text{inv}(\omega))) = \text{int}(\omega)$ . Since  $\widehat{C}_0$  is non-singular, one of the ovals  $\omega$  and  $\text{inv}(\omega)$  is contained in the interior part of the other, and therefore  $\text{inv}$  permutes the ovals  $\omega_0, \dots, \omega_p$ . We get the thesis simply observing that, for all  $i$ ,  $\text{inv}$  transforms  $\text{int}(\omega_i)$  into the exterior part of  $\text{inv}(\omega_i)$ .

c) is readily proved using the previous arguments. □

By Proposition 4.1, in order to subdivide the set of the connected components of  $\widehat{S}$  into  $\widehat{\mathcal{F}}_1$  and  $\widehat{\mathcal{F}}_2$ , it is sufficient, when passing through the level 0, to compute  $\text{findOvals}(0)$  and  $\text{findOvals}(\text{inv}(P_i))$  for the points  $P_i$  given above in T1. After doing that, as a consequence of Remark 2.3 we know that, if an integer appears in the list  $L(\widehat{\mathcal{F}}_2)$  of the Euler characteristics of the components in  $\widehat{\mathcal{F}}_2$ , it appears an even number of times. It is then sufficient to create a new list of integers as follows: if  $\chi$  appears  $2n$  times in  $L(\widehat{\mathcal{F}}_2)$ , we insert it  $n$  times in the new list. The integers in this new list represent the Euler characteristics of the connected components  $\widehat{T}_{m+1}, \dots, \widehat{T}_q$  in Proposition 2.2 and topologically determine them.

## 5 Final remarks and examples

Although our emphasis was put on the theoretical aspects of the problem, we have in fact developed a preliminary implementation of the algorithm and we were forced to confront some technical problems that we outline below.

The general-case algorithm consists of three main parts: the reduction to the study of a suitable compact affine surface  $\widehat{S}$ , the use of CCA to compute its

topology and finally the reconstruction of the topology of  $S$ . The first and third parts are relatively simple, while the second part is very demanding both for the complexity of its implementation and for its computational cost. Clearly the computational cost of this step is greatly influenced by the degree of the polynomial defining the surface; since studying  $\widehat{S}$  instead of  $S$  doubles the degree of the defining equation, the efficiency of the whole algorithm can be heavily affected. Therefore, in order to obtain a satisfactory implementation, very sophisticated tools should be used.

The most delicate steps from this point of view are certainly the non-singularity test, the non-degeneracy test for the real critical points, the computation of the real critical points and values and the lifting of the needed system of data from one level to the next one in the iterative procedure.

The first two tasks require to decide whether the real zero-set  $V_{\mathbb{R}}(I)$  of an ideal  $I$  of  $\mathbb{R}[x, y, z]$ , possibly 1-dimensional, is empty, distinguishing between the real and complex solutions of the corresponding polynomial system. Taking advantage of the low dimension and the specific geometric features of our situation, we used a special purpose method, based on Gröbner bases and a related structure theorem for 1-dimensional ideals, which is described in Fortuna et al. (2003) and Fortuna, Gianni, Parenti (2003). Hence these tasks can be completely performed with exact arithmetic.

Instead, for the computation of the critical points and for the lifting process, the difficulties that arise are mainly of numerical nature. We need to compute the critical points with very high precision, thus this part of the algorithm needs highly optimized software. An accurate complexity analysis of the numerical aspects, though, was out of the scope of this paper, so we defer such a study to further research.

**Example 1.** Let  $F(x, y, z, t) = -z^3 + (y + x - 4t)z^2 + (-y^2 - 2yt - x^2 + 8xt + 2t^2)z + y^3 + (x - 6t)y^2 + (x^2 - 10xt + 10t^2)y + x^3 - 16x^2t + 70xt^2 - 65t^3$ .

The projective surface  $S$  defined by the homogeneous equation  $F(x, y, z, t) = 0$  is non-singular. Since the degree of  $F$  is odd, surely  $S$  intersects the line  $L = \{z = t = 0\}$  in at least one real point, so that the Compact-Case-Algorithm cannot be applied to  $S$ . Thus we consider the compact 6-degree surface  $\widehat{S}$  in  $\mathbb{R}^3$  defined by  $G(x, y, z) = F(2x, 2y, 2z, x^2 + y^2 + z^2 - 1) = 0$  and compute its topology.

The restriction to  $\widehat{S}$  of the projection  $p(x, y, z) = z$  turns out to be a Morse function having 6 distinct critical values, respectively of index 0, 0, 0, 2, 2, 2, contained in the interval  $[-3, 3]$ . This interval is then subdivided as  $[-3, a_1] \cup [a_1, a_2] \cup [a_2, 0] \cup [0, a_4] \cup [a_4, a_5] \cup [a_5, 3]$  (i.e. we can choose  $a_3 = 0$ ) in such a way that each subinterval contains exactly one critical value in its interior part.

The algorithm iteratively reconstructs the topology of the level surfaces  $\widehat{S}_{a_i}$ ;

in particular, when passing through the level  $a_3 = 0$ , it gives us the following additional information:

a) the function `nestsZero` returns the list  $[[P, [\omega_2, \omega_1]], [Q, [\omega_3]]]$ . Thus we recognize that the level curve  $\widehat{C}_0$  contains two nests: the first consists of two ovals  $\omega_2$  and  $\omega_1$  with  $P$  a point internal to both ovals; the second nest contains a single oval  $\omega_3$  containing the point  $Q$ ,

b) the output of the function  `$\mu_0$`  tells us that  $\omega_1, \omega_2, \omega_3$  are contained in 3 distinct connected components of  $\widehat{S} \cap \{z \leq 0\}$ .

When the Compact-Case-Algorithm stops, we see that  $\widehat{S}$  has 3 connected components, each having Euler characteristic 2, i.e. each is a sphere. Moreover there was no gluing of surface components passing through the critical values  $> 0$  (which is obvious since in this example there is no critical value of index 1).

In order to compute the topological type of  $S$  we need to split  $\widehat{\mathcal{F}} = \{\widehat{T}_1, \widehat{T}_2, \widehat{T}_3\}$  into  $\widehat{\mathcal{F}}_1 \cup \widehat{\mathcal{F}}_2$ . First of all, using Proposition 4.1, the algorithm computes the ovals  $inv(\omega_1), inv(\omega_2), inv(\omega_3)$  corresponding through inversion to the ovals  $\omega_1, \omega_2, \omega_3$  of the curve  $\widehat{C}_0$ . Since  $findOvals(0) = [\omega_1]$ , then  $inv(\omega_1) = \omega_1$ . Moreover since  $findPoint(\omega_2) = P$  and  $findOvals(inv(P)) = [\omega_3]$ , then  $inv(\omega_2) = \omega_3$  and  $inv(\omega_3) = \omega_2$ .

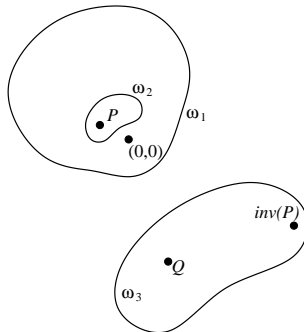


Fig. 4. The shape of the curve  $\widehat{C}_0$  in Example 1

As a consequence of the criterion given in Proposition 2.5, we get that  $\widehat{\mathcal{F}}_1 = \{\widehat{T}_1\}$  and  $\widehat{\mathcal{F}}_2 = \{\widehat{T}_2, \widehat{T}_3\}$ . Coming back to the surface  $\widehat{S}$ , we have that  $\mathcal{F}_1 = \{\widetilde{T}_1\}$  and  $\mathcal{F}_2 = \{\widetilde{T}_2, \widetilde{T}_3 = ap(\widetilde{T}_2)\}$ , where  $\widetilde{T}_i$  is a sphere for  $i = 1, 2, 3$ . Then, by Proposition 2.2,  $S$  is homeomorphic to the disjoint union of  $M(\frac{\chi(\widetilde{T}_1)}{2}) = M(1)$  and  $\widetilde{T}_2$ . Thus  $S$  has two connected components: one of them is a projective plane and the other one is a sphere.

**Example 2.** Let  $S$  be the projective surface defined by  $F(x, y, z, t) = 2yz^2 - (4y^2 + 2xy + 2yt)z + 5y^3 + (4x + 7t)y^2 + (x^2 + 4xt - t^2)y + x^2t - 2xt^2 + t^3 = 0$ .  $S$  is non-singular and intersects the line  $L$ , so we preliminarily study the compact 6-degree surface  $\widehat{S} \subset \mathbb{R}^3$ .

The CCA algorithm computes 6 distinct critical values of index 0, 1, 1, 1, 1, 2 contained in the interval  $[-4, 4]$  and subdivides it as  $[-4, -1] \cup [-1, -\frac{6881}{32768}] \cup [-\frac{6881}{32768}, 0] \cup [0, \frac{2817}{8192}] \cup [\frac{2817}{8192}, 1] \cup [1, 4]$ .



The level surface  $\widehat{S}_{-1}$  is topologically a disc; then we successively pass through four critical values of index 1, that CCA investigates as explained in Section 3. So we see that both in  $[-1, -\frac{6881}{32768}]$  and in  $[0, \frac{2817}{8192}]$  a 1-cell is attached to a single oval, which splits into two ovals; in the first interval the two new ovals form a nest (so we are in case (B1) of Figure 2), while in the second interval the two ovals are each external to the other (so we are in case (A1)). On the contrary in both intervals  $[-\frac{6881}{32768}, 0]$  and  $[\frac{2817}{8192}, 1]$  a 1-cell is attached to distinct ovals that are glued together. Figure 5 shows some sections of  $\widehat{S}$  at different levels

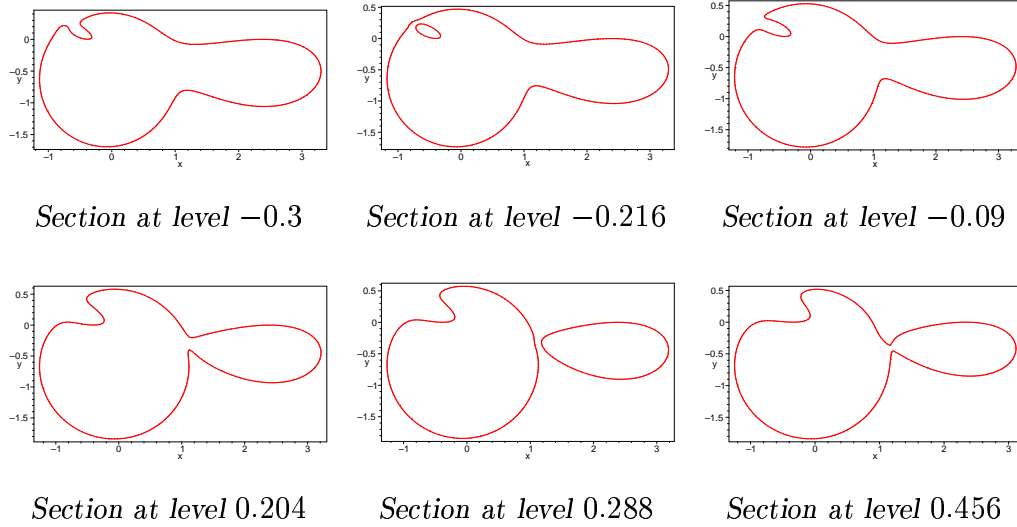


Fig. 5. Some sections of the surface  $\widehat{S}$  of Example 2

Eventually we get that  $\widehat{S}$  is connected and its Euler characteristic is  $-2$ , that is  $\widehat{S}$  is a torus with 2 holes. Necessarily  $\widehat{\mathcal{F}}_1 = \{\widehat{S}\}$  and  $\widehat{\mathcal{F}}_2 = \emptyset$ . By Proposition 2.2,  $S$  is homeomorphic to  $M(\frac{\chi(\widehat{S})}{2}) = M(-1)$ , that is  $S$  is the connected sum of a projective plane and a torus.

**Example 3.** The projective surface  $S$  defined by  $F(x, y, z, t) = z^4 - 8xz^3 + 2(y^2 + 7x^2 + t^2)z^2 + 8(x^3 - xy^2 - xt^2)z + y^4 + 2(7x^2 + t^2)y^2 - 15x^4 - 2x^2t^2 + t^4 = 0$  is non-singular and intersects the line  $L = \{z = t = 0\}$ . So we start to study the 8-degree affine surface  $\widehat{S}$  obtained in the usual way. The projection  $p$  has 8 non-degenerate critical points on  $\widehat{S}$  respectively of index  $0, 0, 1, 1, 1, 1, 2, 2$  and the corresponding 8 critical values are contained in the interval  $[-5, 5]$ .

When studying the level surface  $\widehat{S} \cap \{z \leq 0\}$ , the algorithm output tell us that a)  $nestsZero = [[P, [\omega_1]], [Q, [\omega_2]]]$ , i.e.  $\widehat{C}_0$  contains two ovals  $\omega_1$  and  $\omega_2$  each external to the other,

b)  $\mu_0(\omega_1) \neq \mu_0(\omega_2)$ , that is  $\omega_1$  and  $\omega_2$  bound two distinct connected components of  $\widehat{S} \cap \{z \leq 0\}$ .

At the end of the iterative steps of CCA, we see that  $\widehat{S}$  has 2 connected components  $\widehat{T}_1$  and  $\widehat{T}_2$  each having Euler characteristic 0, i.e.  $\widehat{S}$  consists of two tori. We also see that  $\omega_1$  and  $\omega_2$  are respectively contained in  $\widehat{T}_1$  and  $\widehat{T}_2$ . Since 0 is

external both to  $\omega_1$  and to  $\omega_2$  and  $\text{findOvals}(\text{inv}(P)) = [\omega_2]$ , then  $\text{inv}(\omega_1) = \omega_2$  and  $\text{inv}(\omega_2) = \omega_1$ . Thus we recognize that  $\widehat{\mathcal{F}}_1 = \emptyset$  and  $\widehat{\mathcal{F}}_2 = \{\widehat{T}_1, \widehat{T}_2\}$ ; therefore  $S$  is homeomorphic to  $\widehat{T}_1$ , that is to a torus.

**Example 4.** The non-singular surface  $S$  defined by the homogeneous equation  $(y - 2x)z^2 + y^3 - (4x^2 + t^2)y + 2xt^2 - 4t^3 = 0$ , being of odd degree, intersects the line  $L$ . Computations yield that its “doubled” surface  $\widehat{S}$  is connected, with Euler characteristic 2, i.e. it is a sphere. Then necessarily  $\widehat{\mathcal{F}}_1 = \{\widehat{S}\}$  and  $\widehat{\mathcal{F}}_2 = \emptyset$ ; hence  $S$  is homeomorphic to  $M(\frac{\chi(\widehat{S})}{2}) = M(1)$ , that is  $S$  is topologically a projective plane.

## References

- Fortuna, E., Gianni, P., Parenti, P. and Traverso, C. Algorithms to compute the topology of orientable real algebraic surfaces, *J. Symbolic Comput.*, vol. 36, n. 3-4 (2003), pp. 343-364
- Fortuna, E., Gianni, P. and Parenti, P. Some constructions for real algebraic curves. *Pubbl. Dip. Mat. Univ. Pisa*, 1.285.1441 (2003).
- Hirsch, M. W. *Differential topology*. Springer-Verlag, New York, 1976. Graduate Texts in Mathematics, No. 33.
- Massey, W. S., *A basic course in algebraic topology*. Springer-Verlag, New York, 1991.
- Milnor, J. *Morse theory*. Princeton University Press, Princeton, N.J., 1963.
- Viro, O., Mutual position of hypersurfaces in projective space. *Amer. Math. Soc. Transl. Ser. 2*, vol. 186, (1998), pp. 161–176